17th World Conference on Earthquake Engineering, 17WCEE
Sendai, Japan - September 13th to 18th 2020

Distribution Characteristics of Wave Pressure on Buildings Subjected to Tsunami Load

A. Obata[(1)], T. Nishida[(2)]

[(1)] *Assistant Professor, Akita Prefectural University, a_obata@akita-pu.ac.jp*
[(2)] *Professor, Akita Prefectural University, tetsuya_nishida@akita-pu.ac.jp*
…

Abstract

On March 11, 2011, an earthquake occurred off the Pacific coast of Tohoku. The tsunami caused by this earthquake resulted in severe and extensive structural damage in Northeastern Japan. In light of such events, the establishment of a new high-accuracy tsunami resistance design method for buildings is an urgent issue in the academic field of building structural engineering. In order to achieve structural designs of buildings that can withstand tsunami loads, it is necessary to quantitatively evaluate the tsunami load exerted on these buildings. At this point, however, there are very few examples of quantitative evaluation, analysis, or estimation related to tsunami loads in the building structural engineering field.

The purpose of this study is to clarify the distribution characteristics of tsunami wave pressure on buildings subjected to tsunami loads. In recent years, the Architectural Institute of Japan has included a new chapter on tsunami loads in the "AIJ Recommendations for Loads on Buildings (2015)". [1] Because of the large impact of the tsunami damage resulting from the previous earthquake on building owners, the number of cases in which designers are required to explain the safety of buildings against tsunamis has increased. The "AIJ Recommendations for Loads on Buildings (2015)" has been established as a design guideline, incorporating knowledge from the field of coastal engineering; this guideline is accepted by designers as an index and used as an explanation tool for owners. However, there are many problems caused by diverting knowledge from the field of coastal engineering to building structures. Although many of these problems are overdesigned, they are omitted in the load guidelines because they are precautionary in nature. Therefore, it is necessary to organize these design guidelines.

General civil engineering structures are large structures that include revetments and tide walls. The problem, therefore, is how much and at which heights such structures are subjected to tsunami horizontal forces. These building structures are comprised of structural members in layers. The strength in the horizontal direction of each building structure is defined by the shear strength of each layer. In the structural design, the distribution characteristics of wave pressure on building surfaces must therefore be considered for the assessment of horizontal loads such as tsunamis.

In this study, hydraulic experiments are conducted to understand the distribution characteristics of tsunami wave pressure acting on the front of these structures. In these hydraulic experiments, the horizontal force as the total amount of tsunami load has been also evaluated in order to consider the qualitative and quantitative tendencies of the tsunami load that the building structure is subjected to.

Keywords: Tsunami Load; Tsunami Pressure, Distribution Characteristics of Wave Pressure; Hydraulic Experiments

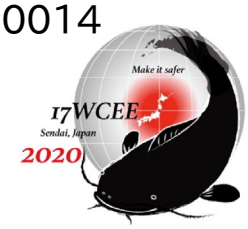

1. Introduction

Published research on tsunami load has been actively focused mainly on coastal engineering structures. In general, coastal engineering structures refer to large and homogeneous constructions, such as seawalls. For structures such as these, the tsunami load is often considered as a horizontal force. The problem is determining at which point and how much of this force to which these structures are subjected. On the other hand, these building structures are composed of layered elements, some of which support the living space on each floor with vertical members, such as columns or walls, and others which connect the column heads, such as beams or slabs. The horizontal strength of the building structure is assumed from the shear strength of each of the stories. Therefore, in structural design, determining the relationship between the strength of each of the stories and the shear force calculated from the external load is necessary.

In a previous survey of the tsunami damage caused by the earthquake off the Pacific coast of Tohoku on March 11, 2011, a case has been reported of a two-story steel building, which, although the first story was inelastic, had collapsed at the second story.[2] In this building as an example, it cannot be explained if the triangular wave pressure distribution of tsunami load, assumed to be the structural requirement in Notification No. 1318 of the Japanese Ministry of Land, Infrastructure, Transport and Tourism[3] et al., had been followed. Designing for tsunami loads requires careful consideration of the pressure distribution characteristics on the tsunami-receiving surface.

In this study, hydraulic experiments are conducted to understand the distribution characteristics of tsunami wave pressure acting on the front surfaces of these structures. In these hydraulic experiments, the horizontal force, as the total amount of tsunami load, has also been evaluated to consider the qualitative and quantitative tendencies of the tsunami load to which the building structure is subjected.

2. Outline of hydraulic experiments

2.1 Test channel and models

In this study, hydraulic experiments are done in the National Institute of Technology, Akita College. Fig. 1 shows an outline of the test channel. The test channel is 15 m long, 0.6 m wide, and 0.8 m deep. The water gate is set 4.0 m above the upper side of the channel. The tsunami waves are reproduced by storing water in the water tank and opening the water gate. The wave absorber is installed at the lower end of the test channel, and the tsunami water is drained to a floor drain near the wave absorber. In this test, a small reflection wave of tsunami is generated by the wave absorber. The test model is set at a position 6.5 m from the water gate, and tsunami wave force and pressure are observed until the time when the reflection wave reaches the test model.

For simplicity, the building structure used for the test model is assumed to be a rectangular structure without openings such as windows. The test model, made of an acrylic plate, has a square plane shape. Model 1 has a width × depth of 120 mm × 120 mm, whereas model 2 has a width × depth of 80 mm × 80 mm. The blockage ratios of model 1 and model 2 are 0.20 and 0.16, respectively. The height of the test model, for both models, is 120 mm. In this test, the magnitude of the tsunami is adjusted by changing the amount of water stored in the water tank. Storing water depth h_w is set for four cases (h_w = 100 mm, 140 mm, 180 mm, 220 mm).

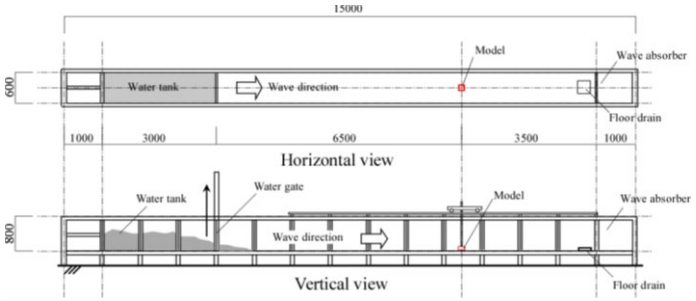

Fig. 1 – Outline of test channel

2.2 Model setting and measurement

In this experiment, the flow velocity in front and back of the model, wave height in front and back of the model, wave force acting on the model, and wave pressure on the front surface of the model are measured. Fig. 2 shows the outline of the model setting, and Fig. 3 shows the outline of the measurement device arrangement. The flow velocity in front and back of the model is measured by the velocity meters. The wave height in front and back of the model is measured by the height gauges.

The model is fixed to the tip of the steel plate. The steel plate is hung on the truck that is setting above the model position. A 5.0mm clearance is provided between the model and the channel floor. When the model receives the tsunami wave, the model does not contact the floor of the channel. Thus, the tsunami load is the wave force acting on the model in tsunami mainstream direction, and the wave force is measured from the bending moment subjecting on the steel plate. The tsunami pressure is wave pressure applied to a local area, and the wave pressure is measured by the pressure gauge embedding on front surface of the model. Fig. 4 shows the position of the pressure gauges. The pressure gauges are installed at three vertical levels, named top, middle and bottom. The distance between channel floor and each levels is 20mm. The pressure gauges at top and middle levels were installed two axes, center and right. The pressure gauges at bottom levels were installed three axes, left, center and right. Three cases were prepared for model 1, and two cases were prepared for model 2 at the distance from the center axis to the left and right axis. There were numbered as shown in figure. The sampling frequency is 100 Hz

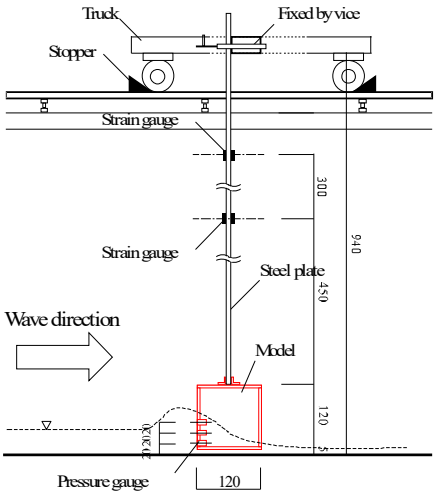

Fig. 2 – Outline of the model setting

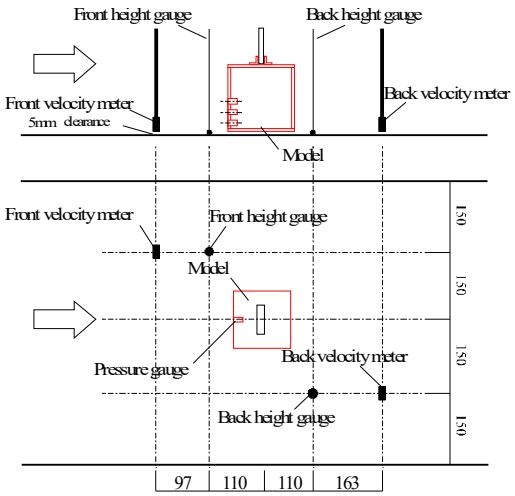

Fig. 3 – Outline of the measurement device arrangement

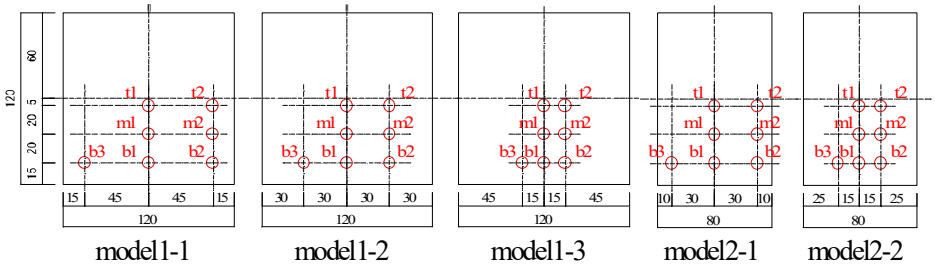

Fig. 4 – Positions of the pressure gauges

3. Preliminary experiment

3.1 Outline of preliminary experiment

In a preliminary experiment, which is conducted to confirm the properties of the tsunami wave in this experiment channel, the flow velocity and wave height are measured without the experimental model installed in the set-up. The experimental parameter is the storing water height h_w. For this preliminary experiment, the velocity meters and wave height gauges are installed as shown in Fig. 3, such that they are aligned with respect to the front and back of the tsunami flow. Therefore, the front height gauge is affected by the front velocity meter. Similarly, the back velocity meter is also affected by the back height gauge. Thus, the value of there is measured small. Because confirming the characteristics of the wave at each storing water height in an undisturbed state is necessary, the flow velocity in the preliminary experiment is considered to be equivalent to the value obtained by the front velocity meter, and the wave height is considered to be equivalent to the value obtained by the back wave height meter. For each storing water height, the preliminary experiment is performed five times.

3.2 Dispersion in experimental results depending on the number of experiments

As examples, five flow velocity–time histories at storing water heights h_w = 100 mm and 220 mm are shown in Fig. 5. The measurement start time (time 0.0 s) of the time histories is defined as 1.0 s before the start of data recording by the front velocity meter. Hereafter, in this paper, the measurement start time of the time histories is defined in the same way. As shown in Fig. 5, differences in the maximum value occur five times, but otherwise, there is no general difference in the tendencies. In Fig. 5, the red line shows the ensemble average value for five time histories. The ensemble average value, which is almost the median of the results of the five tests, suggests the tendency of the experimental results. Hereafter, in this paper, the results of the experiments in each case is represented by the ensemble average of five tests.

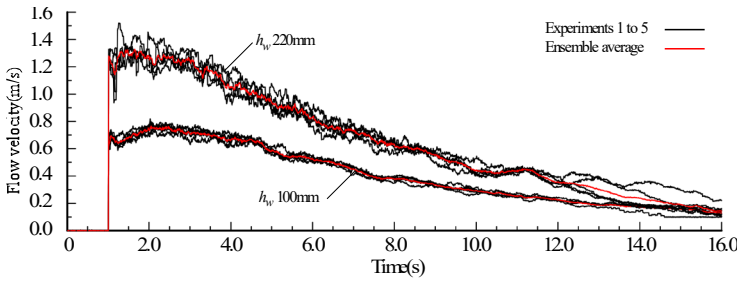

Fig. 5 – five flow velocity–time histories

3.3 Time histories of flow velocity, wave height, and Froude number without experimental model

Fig. 6, Fig. 7, and Fig. 8 show the time histories of the flow velocity, wave height, and Froude number, respectively, of the preliminary experiment at each h_w. The flow velocity, wave height, and Froude number exhibit larger values as h_w increases. The flow velocity exhibits the maximum value immediately after the start of recording, whereas the wave height exhibits the maximum value slightly later. The time when the flow velocity exhibits maximum value is confirmed to not coincide with the time when the wave height exhibits the maximum value. In the time history of the Froude number, there is a segment of time in which the Froude number is recorded to be extremely high immediately after the start of recording. This phenomenon occurs because the wave arrives at the flow velocity meter earlier than at the wave height gauge, and thus there is a segment of time where only the flow velocity is recorded. These segments of time are therefore excluded from consideration. In the case of h_w = 220 mm, the Froude number gradually decreases from around 2.0 with the lapse of time, and in the case of h_w = 100 mm, the Froude number also gradually decreases from around 1.5 with the lapse of time. In all cases, the wave switches from supercritical flow to subcritical flow between about 6.0 and 8.0 seconds.

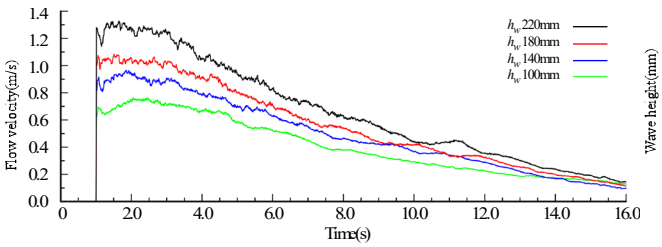

Fig. 6 –Time histories of the flow velocity

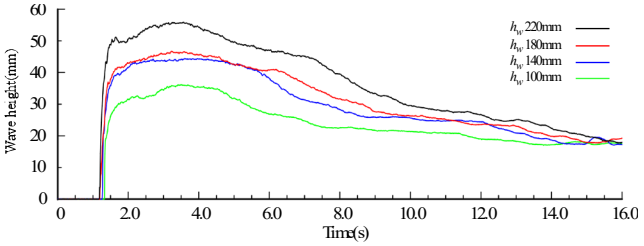

Fig. 7 – Time histories of the wave height

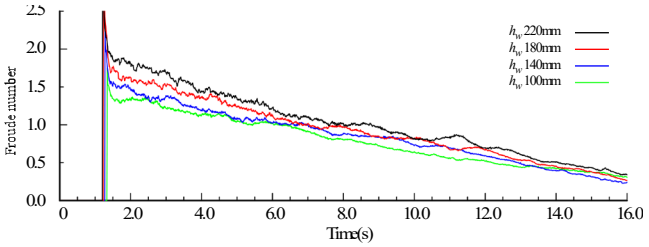

Fig. 8 –Time histories of the Froude number

4. Results

4.1 Time histories of flow velocity, wave height, and wave force

The time histories of flow velocity, wave height, and wave force for model l and model 2 are shown in Fig. 9 and Fig. 10, respectively. In each of the time histories of flow velocity and wave height, the measured value at the front of the model is indicated by a solid line, whereas the measured value at the back of the model is indicated by a broken line. In each of the time histories of wave force, the measured value obtained by the strain gauge attached to the steel plate is indicated by a solid line, whereas the calculated wave force F_{eq} is indicated by a broken line. The calculated wave force F_{eq} is determined as follows:

$$F_{eq} = \frac{1}{2} C_D \rho v_f^2 B (h_f - \phi) + \frac{1}{2} \rho g B \{(h_f - \phi)^2 + (h_b - \phi)^2\}, \quad (1)$$

where, C_D : drag coefficient of the rectangular section column, ρ : water density (= 1.0 ton / m^3), v_f : flow velocity at the front of the model (m/s), B : width of the model (m), h_f : wave height at the front of the model (m), h_b : wave height at the back of the model (m), and ϕ : clearance between the model and channel floor (= 0.005 m). The drag coefficient of rectangular section column C_D is set to 1.2, referring to the wind coefficient at the time of the wind load design. It is a debatable point. In equation (1), the first item on the right side represents the wave force due to dynamic pressure, whereas the second item on the right side represents the wave force due to static pressure. The drag coefficient C_D included in the first item on the right side in equation (1) is the sum of the drag coefficients at the front and back of the structure. With the second item on the right side, the horizontal force generated in the structure due to the difference in wave heights between the front and back of the structure is represented. Therefore, equation (1) is said to be an equation that includes the influence of the back of the structure.

From Fig. 9 and Fig. 10, the values of the flow velocity, wave height, and wave force are confirmed to have increased as h_w increased. The values of the flow velocities at the front and back of the model exhibit maximum values immediately after the start of data recording. The flow velocity at the front side then rapidly decreases, whereas the flow velocity at the back of the model gradually decreases with the lapse of time. For the wave height, the maximum value is reached shortly after the start of data recording because of stagnation at the front of the model. When the flow velocity exhibits its maximum value, the value of the wave height is low. By contrast, when the wave height exhibits its maximum value, the value of the flow velocity is low. In this experiment, the wave force is confirmed to reach its maximum value near the time when the wave height reaches its maximum for model1 and near the time when the flow velocity becomes

maximum for model 2. In the time history of the wave force, from time = 1.0 s to 6.0 s, the wave force F_{eq} calculated from equation (1) exceeds the wave force measured from the strain gauges. However, after time = 6.0 s, F_{eq} demonstrates a good correspondence with the measured wave force. In this experiment, after time = 6.0 s, the Froude number F_r is considered to be less than 1.0, and the flow field is considered to be equivalent to subcritical flow, as shown in Fig. 5. Therefore, the wave force calculated using equation (1) is said to be good under subcritical flow.

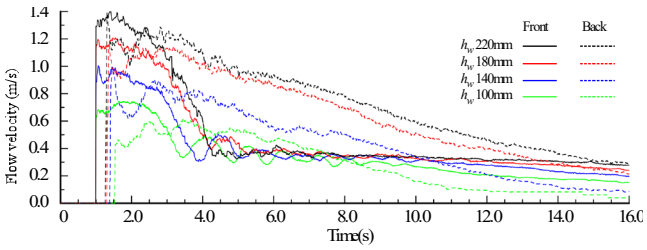

(1) Time histories of flow velocity

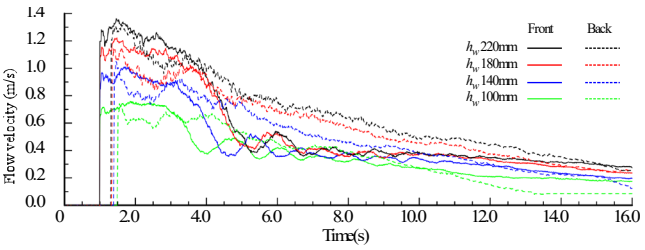

(1) Time histories of flow velocity

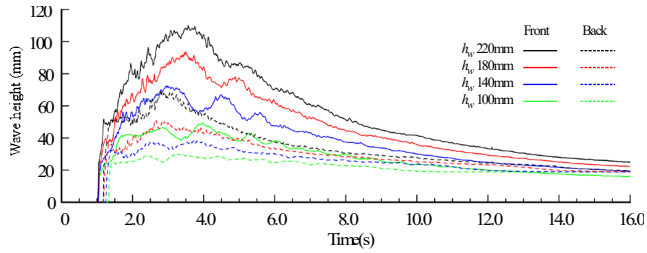

(2) Time histories of wave height

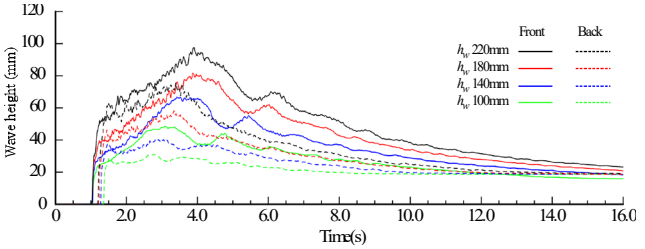

(2) Time histories of wave height

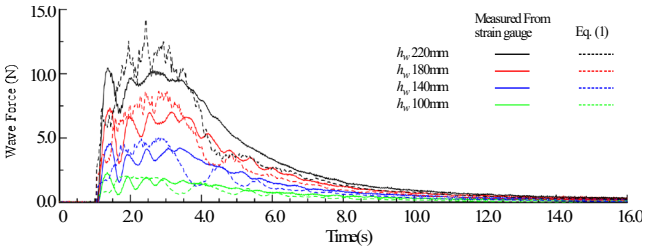

(3) Time histories of wave force

Fig. 9 –Time histories of flow velocity, wave height, and wave force in model1

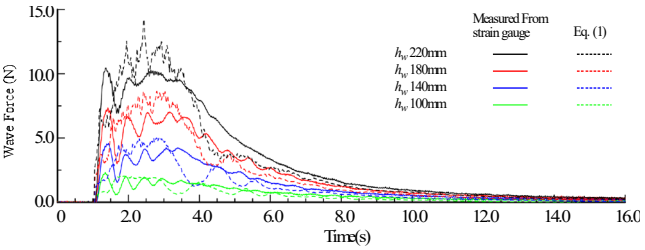

(3) Time histories of wave force

Fig. 10 – Time histories of flow velocity, wave height, and wave force in model2

4.2 Time history of wave pressure

Fig. 11 shows the time history of the wave pressure of each model at h_w = 180 mm, whereas Fig. 12 shows the water pressure at h_w = 220 mm. The same qualitative tendency is shown in the case of h_w = 100 mm and 140 mm, although the value is smaller. To verify the wave pressure from the pressure gauge, the wave pressure at the pressure gauge position is calculated using the experimental values of the flow velocity and wave height. The calculated wave pressure p_{eq} is determined as follows:

$$p_{eq} = \frac{1}{2} C_D \rho v_f^2 + \rho g (h_f - z_i), \quad (2)$$

where, C_f : drag coefficient on the front surface of the structure, and z_i : height (m) from the channel floor to the pressure gauge (m). The drag coefficient C_f on the front surface of the structure is set to 0.8, referring to the wind coefficient at the time of the wind load design. It is a debatable point. According to Fig. 11 and Fig. 12, the calculated wave pressure is generally better than the measured wave pressures at the top and middle

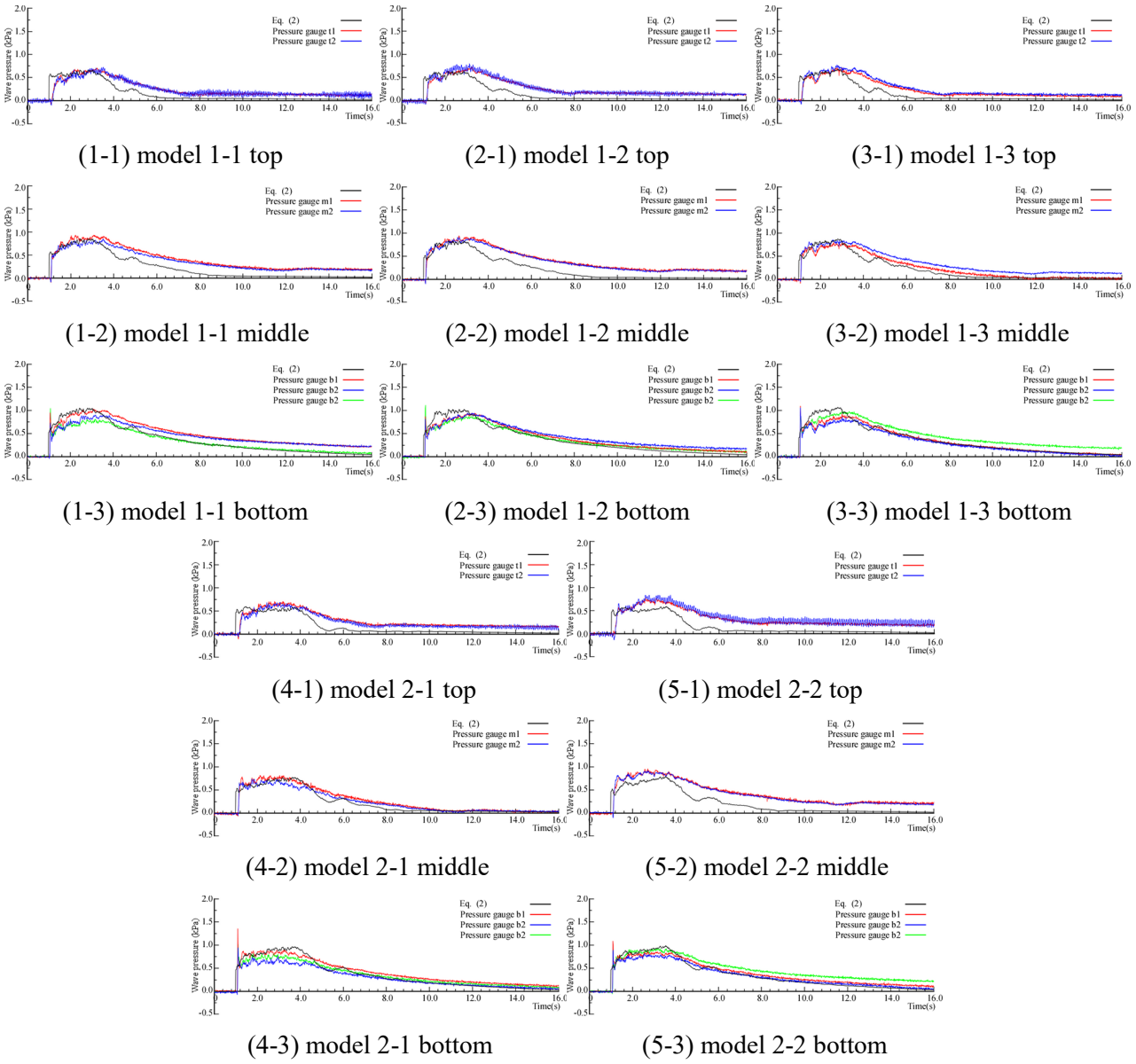

(1-1) model 1-1 top (2-1) model 1-2 top (3-1) model 1-3 top

(1-2) model 1-1 middle (2-2) model 1-2 middle (3-2) model 1-3 middle

(1-3) model 1-1 bottom (2-3) model 1-2 bottom (3-3) model 1-3 bottom

(4-1) model 2-1 top (5-1) model 2-2 top

(4-2) model 2-1 middle (5-2) model 2-2 middle

(4-3) model 2-1 bottom (5-3) model 2-2 bottom

Fig. 11– Time histories of wave pressure (h_w = 180 mm)

levels. The measured wave pressure from the pressure gauge at the bottom level, on the other hand, exhibits a slightly lower value than that of the calculated wave pressure, because the pressure did not rise sufficiently because of the flow of water through the 5 mm clearance below the model.

Separately, an experiment is conducted in which the clearance is filled, and as a result, the pressure demonstrates a good correspondence with the calculated wave pressure. Although there are some exceptions, for the wave pressure measured from the pressure gauge at the bottom and middle levels, the pressure values at the center of the model (m1, b1) are generally the highest, whereas the pressure values at the right side of the model (m2, b2) are almost the same or slightly lower than the values at the center. This effect is especially remarkable in model 1-1 and model 2-1, where the right side of the measurement position (m2, b2) is nearest to the model edge. From these results, with regard to the horizontal distribution of wave pressure, the wave pressure value at the model edge is low. The pressure is observed not to increase at the model edge because the water flow escapes to the side of the model. On the other hand, the wave pressure at

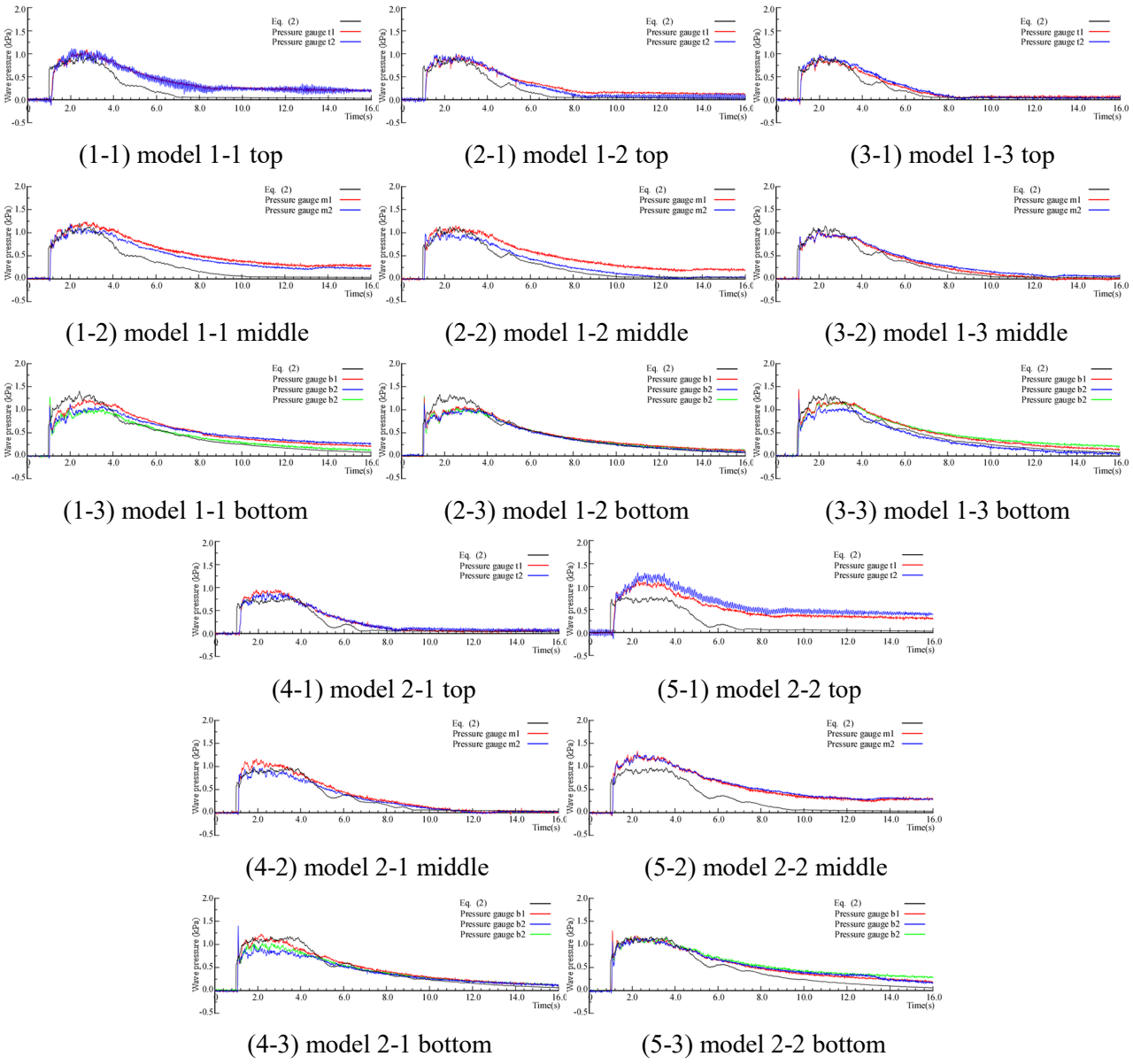

(1-1) model 1-1 top (2-1) model 1-2 top (3-1) model 1-3 top

(1-2) model 1-1 middle (2-2) model 1-2 middle (3-2) model 1-3 middle

(1-3) model 1-1 bottom (2-3) model 1-2 bottom (3-3) model 1-3 bottom

(4-1) model 2-1 top (5-1) model 2-2 top

(4-2) model 2-1 middle (5-2) model 2-2 middle

(4-3) model 2-1 bottom (5-3) model 2-2 bottom

Fig. 11– Time histories of wave pressure (h_w = 220 mm)

the top level is confirmed to be almost similar to the pressures at both the center and the model edge. In other words, this effect is small at the top level.

5. Conclusion

In this study, hydraulic experiments were conducted to understand the distribution characteristics of tsunami wave pressure acting on the front surfaces of these structures. According to the results of the experiment, the wave pressure demonstrates a good correspondence with the calculation studied in this report. Furthermore, regarding the horizontal distribution of wave pressure, the wave pressure value at the model edge is low. The pressure did not increase at the model edge because the water flow escaped to the side of the model. In this study, a rough qualitative trend of wave pressure generated in a building structure subjected to a tsunami was observed. However, to use the tsunami wave pressure for building structural designs, a more detailed examination of the wave pressure distribution characteristics is necessary.

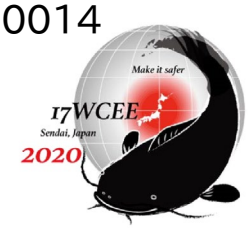

Acknowledgements

The authors are deeply grateful to Associate Prof. N. Teramoto and his Team of the National Institute of Technology, Akita College for his help on the laboratory tsunami test.

References

[1] Architectural Institute of Japan (2015): *AIJ Recommendations for Loads on Buildings*.

[2] Syuji T (2012): Damage caused by the tsunami of the Great East Japan Earthquake. *Annuals of Disas. Prev. Res. Inst. Kyoto Univ.,* No. 55A, (in Japanese).

[3] Japanese Ministry of Land, Infrastructure, Transport and Tourism (2011): Notification No. 1318 of the Japanese Ministry of Land, Infrastructure, Transport and Tourism.

[4] Cabinet Office (2017): *Promotion of Tsunami Disaster Prevention Measures Utilizing Tsunami Evacuation Buildings.*

[5] Hitoshi K (2016): Drag and Uplift of a Cuboid Structure Standing in Inundation Flow, Hydraulic study in natural river flow Part 2, *Journal of Structural and Construction Engineering, Architectural Institute of Japan, Vol. 81, No.* 720, pp. 219-228

[6] Akihiko O, Tetsuya N (2017): Hydraulic Experiments of Flow Behind a Cubical Structures under Overflow Tsunami, *Proceedings of Annual Meeting of Tohoku Chapter, Architectural Institute of Japan,* Part 80, pp. 87-90, (in Japanese).

[7] Akihiko O, Tetsuya N (2018): Hydraulic Experiments of Flow Behind a Cubical Structures under Overflow Tsunami, Part2 : Consideration on the shape of structure, *Proceedings of Annual Meeting of Tohoku Chapter, Architectural Institute of Japan,* Part 81, pp. 117-120, (in Japanese).

[8] Akihiko O, Naofumi T, Tetsuya N (2019): An Experimental Study on Wave Pressure behind a Cubical Structures due to Overflowing Tsunami, *Proceedings of Annual Meeting of Tohoku Chapter, Architectural Institute of Japan,* Part 81, pp., (in Japanese).

